Arch Pharm Res Vol 35, No 8, 1393-1401, 2012
DOI 10.1007/s12272-012-0809-0

Archives of Pharmacal Research
www.springer.com/12272

N-Methylthioureas as New Agonists of Retinoic Acid Receptor-Related Orphan Receptor

Yohan Park[1], Suckchang Hong[2], Myungmo Lee[2], Hyojun Jung[2], Won-Jea Cho[3], Eun-Jin Kim[4], Ho-Young Son[4], Mi-Ock Lee[4], and Hyeung-geun Park[2]

[1]College of Pharmacy, Inje University, 607 Obang-dong, Gimhae, Gyeongnam 621-749, Korea, [2]Research Institute of Pharmaceutical Sciences and College of Pharmacy, Seoul National University, Seoul 151-742, Korea, [3]College of Pharmacy Chonnam National University, Kwangju 500-757, Korea, and [4]Bio-MAX Institute and College of Pharmacy, Seoul National University, Seoul 151-742, Korea

(Received March 15, 2012//Accepted April 12, 2012)

Thirty two thiourea derivatives were prepared and their agonistic activities on the retinoic acid receptor-related orphan receptor α (RORα) were evaluated. The replacement of the 3-allyl-2-imino-thiazolidin-4-one moiety of the lead compound CGP52608 (**1**) with various functional group substituted aromatic rings, improved the agonistic activity of RORα. Among the prepared derivatives, 1-methyl-3-(4-phenoxy-benzyl)-thiourea (**32**) showed 2.6-fold higher agonistic activity than CGP52608 in the RORα-activation assay.

Key words: Thiourea derivatives, Agonists, Retinoid acid receptor-related orphan receptor α, CGP52608

INTRODUCTION

Retinoic acid related-receptor orphan receptors, RORα (Becker-Andre et al., 1993; Giguere et al., 1994, 1995), RORβ (Carlberg et al., 1994), and RORγ (Hirose et al., 1994; Ortiz et al., 1995; Medvedev et al., 1996; He et al., 1998; Jetten et al., 2001; He, 2002; Jetten and Ueda, 2002; Eberl and Littman, 2003), are transcription factors belonging to the steroid hormone receptor superfamily. These receptors have been regarded as critical factors in the regulation of a number of physiological processes (Jetten, 2004). Among the receptors, RORα plays an important role in the development of the cerebellum by regulating Purkinje cell differentiation and proliferation of granule cell progenitors (Gold et al., 2003). RORα also plays a role in lipid and steroid metabolism including lipogenesis and fatty acid oxidation (Vu-Dac et al., 1997; Lau et al., 2008), hepatic lipid metabolism (Wang et al., 2010), and homeostasis of cholesterol (Wada et al., 2008). In addition, RORα participates in the maintenance of bone tissue (Meyer et al., 2000). Since those physiological functions of RORα can be possibly modulated by exogenous ligands, the discovery of new non-natural ligands may lead to the development of novel therapeutics for human diseases that involve RORα. In 1995 and 1996, the pineal gland hormone melatonin and thiazolidinone type CGP52608 (**1**), respectively, were identified as efficient agonists of RORα and showed antiarthritic activity *in vivo*, indicating that they may be used as novel therapeutics for the treatment of rheumatoid arthritis and other autoimmune diseases (Steinhilber et al., 1995; Wiesenberg et al., 1995; Missbach et al., 1996). Recent studies on the crystal structure and transcriptional activity of RORα also revealed that cholesterol sulfate is an efficient agonist of RORα (Kallen et al., 2002, 2004). The activated transcription of RORα by cholesterol itself increased apoA-I expression, which carries cholesterol from peripheral cells to the liver to protect against cholesterol accumulation in arterial walls, preventing coronary arteriosclerosis (Vu-Dac et al., 1997; Raspe et al., 2001).

In this paper, we report the synthesis and RORα activity of thiourea derivatives, based on thiazolidinone

Correspondence to: Hyeung-geun Park, Research Institute of Pharmaceutical Sciences and College of Pharmacy, Seoul National University, Seoul 151-742, Korea
Tel: 82-2-880-7871, Fax: 82-2-872-9129
E-mail: hgpk@snu.ac.kr

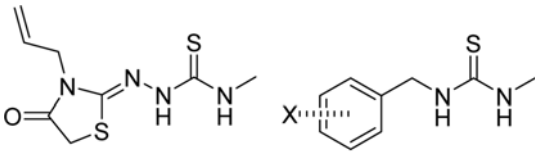

Fig. 1. Structure of CGP52608 (**1**) and N-methyl thiourea analogues (**2**).

type CGP52608 (**1**). As part of our program to develop novel drug-like RORα agonists for the treatment of metabolic disorders such as fatty liver diseases, we chose the first non-natural ligand, CGP52608 (**1**) as a lead compound and attempted to replace the thiazolidin-4-one moiety of **1** with the phenyl rings, substituted with various functional groups. Based on the similarity of the two moieties in size, we assumed that the N-methyl-thiourea analogues (**2**) could retain the agonistic activity against RORα (Fig. 1).

MATERIALS AND METHODS

Chemistry

Organic solvents were concentrated under reduced pressure using a Büchi rotary evaporator. Syringes, needles and cannulae were oven dried at 100°C. TLC analyses were performed using Merck precoated TLC plate (silica gel 60 GF_{254}, 0.25 mm). Flash column chromatography was carried out using E. Merck Kieselgel 60 (230~400 mesh). Infrared (IR) spectra were recorded on a JASCO FT/IR-300E and Perkin-Elmer 1710 FT spectrometer. Nuclear magnetic resonance (^{1}H-NMR and ^{13}C-NMR) spectra were measured on JEOL JNM-LA 300 [300 MHz (^{1}H), 75 MHz (^{13}C)] spectrometer, JEOL JNM-GSX 400 [400 MHz (^{1}H), 100 MHz (^{13}C)] spectrometer, and Bruker AMX 500 [500 MHz (^{1}H), 125 MHz (^{13}C)] spectrometer, using $CHCl_3$-*d*, CH_3OH-*d*, DMSO-*d* as solvents. Nuclear magnetic resonance (^{1}H-NMR and ^{13}C-NMR) spectra using $CHCl_3$-*d* were reported in ppm relative to $CHCl_3$ (δ 7.24) for ^{1}H-NMR and relative to the central $CDCl_3$ (δ 77.23) resonance for ^{13}C-NMR. Nuclear magnetic resonance (^{1}H-NMR and ^{13}C-NMR) spectra using CH_3OH-*d* were reported in ppm relative to CH_3OH (δ 4.87) for ^{1}H-NMR and relative to the central CH_3OH (δ 49.15) resonance for ^{13}C-NMR. Nuclear magnetic resonance (^{1}H-NMR and ^{13}C-NMR) spectra using DMSO-*d* were reported in ppm relative to DMSO (δ 2.50) for ^{1}H-NMR and relative to the central DMSO (δ 39.51) resonance for ^{13}C-NMR. Coupling constants (*J*) in 1H-NMR are in Hz. Low-resolution mass spectra (MS) were recorded on a VG Trio-2 GC-MS spectrometer and mass spectra (MS) were measured on a JEOL JMS-AX 505wA, JEOL JMS-HX/HX 110A spectrometer. Melting points were measured on a Buchi B-540 melting point apparatus and were not corrected.

General procedure

The coupling of methylisocynate with various benzylic amines **3** gave the corresponding N-methylthioureas (**6**-**29**). N-Methyl isothiocyanate (0.15 mL, 2.20 mmol) was added to a stirred solution of substituted benzylamine (1.00 mmol) in diethyl ether or dichloromethane (4 mL). The reaction mixture was stirred sufficiently at ambient temperature until benzylamines were disappeared by TLC analysis. Then the reaction mixture was evaporated and diluted with diethyl ether (100 mL) and filtered to afford N-methylthioureas. The residue was purified by column chromatography (silica gel, hexanes-EtOAc = 3:1 or 1:1) to afford N-methylthioureas (Scheme 1).

The formation of imine from aldehydes **5** and N-methylthiourea in the presence of $Ti(OiPr)_4$ under THF, followed by reduction with $NaBH_4$ provided the corresponding N-methylthioureas (**30**-**36**) (Armstrong et al., 1997). Magnetic bar was added to two-neck round bottom flask and vaccumed. After Ar gas substituted, N-Methyl thiourea (450.8 mg, 5.00 mmol) was added to a stirred solution of substituted benzaldehyde (1.00 mmol) in anhydrous THF (4 mL). Then titanium(IV) isopropoxide (0.50 mL, 1.70 mmol) was added to a reaction mixture. The reaction mixture was refluxed until benzaldehyde were disappeared by TLC analysis. Then the reaction mixture was cooled down to room temperature and $NaBH_4$ (37.8 mg, 1.00 mmol) was added. After stirring for 1 h, neutralized reaction mixture using 1 M HCl. The reaction mixtures was diluted with dichloromethane (50 mL), washed with brine (20 mL), dried over anhydrous $MgSO_4$, filtered, and concentrated *in vacuo*. The residue was purified by column chromatography (silica gel, hexanes-EtOAc = 2:1) to afford N-methylthioureas (Scheme 1).

1-Benzyl-3-methyl-thiourea (6)
White solid; yield 99%; m.p. 89°C; IR (KBr) 3258, 3062, 3029, 2931, 2854, 1954, 1870, 1810, 1657, 1557, 1496, 1453, 1372, 1346, 1293, 1227, 1202, 1173, 1090, 1070, 1028, 959, 742, 697 cm^{-1}; FAB-MS (*m/z*): 181 $[M+H]^+$; ^{1}H-NMR (300 MHz, $CDCl_3$) δ 7.29-7.20 (m, 5H), 6.69 (s, 2H), 4.58 (s, 2H), 2.81 (s, 3H) ppm; ^{13}C-NMR (100 MHz, $CDCl_3$) δ 181.8, 137.0, 128.2, 127.1, 126.9, 47.7, 30.5 ppm.

1-(4-Fluoro-benzyl)-3-methyl-thiourea (7)
White solid; yield 81%; m.p. 92°C; IR (KBr) 3254, 1604,

1557, 1509, 1345, 1296, 1223, 1157, 1081, 1016, 964, 822 cm^{-1}; FAB-MS (*m/z*): 199 $[M+H]^+$; ^{1}H-NMR (300 MHz, CD_3OD) δ 7.35-7.30 (m, 2H), 7.05-6.99 (m, 2H), 4.68 (s, 2H), 2.93 (s, 3H) ppm; ^{13}C-NMR (75 MHz, CD_3OD) δ 165.1, 161.8, 136.1, 130.4, 116.2, 72.0, 31.0 ppm.

1-(3,4-Difluoro-benzyl)-3-methyl-thiourea (8)
White solid; yield 55%; m.p. 122ºC; IR (KBr) 3255, 1611, 1558, 1519, 1437, 1344, 1286, 1210, 1115, 966, 816, 778 cm^{-1}; FAB-MS (*m/z*): 217 $[M+H]^+$; ^{1}H-NMR (400 MHz, DMSO) δ 7.97 (s, 1H), 7.52 (s, 2H), 7.40-7.29 (m, 2H), 7.13 (s, 1H), 4.63 (s, 2H), 2.83 (s, 3H) ppm; ^{13}C-NMR (100 MHz, DMSO) δ 183.7, 150.4, 148.0, 137.6, 123.9, 117.2, 45.8, 30.7 ppm.

1-(2,4-Difluoro-benzyl)-3-methyl-thiourea (9)
Yellow solid; yield 99%; m.p. 119ºC; IR (KBr) 3225, 1569, 1505, 1428, 1375, 1353, 1272, 1231, 1137, 1103, 1078, 966, 859, 746 cm^{-1}; FAB-MS (*m/z*): 217 $[M+H]^+$; ^{1}H-NMR (400 MHz, CD_3OD) δ 7.40 (dd, J_1 = 14.84 Hz, J_2 = 8.00 Hz, 1H), 6.93-6.88 (m, 2H), 4.72 (s, 2H), 2.94 (s, 3H) ppm; ^{13}C-NMR (100 MHz, CD_3OD) δ 165.7, 164.1, 163.3, 161.7, 132.5, 124.0, 112.9, 42.9, 31.5 ppm.

1-(4-Chloro-benzyl)-3-methyl-thiourea (10)
White solid; yield 71%; m.p. 110ºC; IR (KBr) 3255, 3062, 1557, 1492, 1343, 1292, 1091, 1014, 964, 931, 802 cm^{-1}; FAB-MS (*m/z*): 215 $[M+H]^+$; ^{1}H-NMR (300 MHz, $CDCl_3$) δ 7.32-7.24 (m , 4H), 5.96 (s, 2H), 4.68 (s, 2H), 2.96 (d, J = 4.59 Hz, 3H) ppm; ^{13}C-NMR (100 MHz, $CDCl_3$) δ 182.55, 135.71, 133.51, 128.87, 47.69, 30.75 ppm.

1-(3,4-Dichloro-benzyl)-3-methyl-thiourea (11)
White solid; yield 39%; m.p. 136ºC; IR (KBr) 3230, 1557, 1515, 1471, 1299, 1205, 1130, 1030, 961, 824 cm^{-1}; FAB-MS (*m/z*): 249 $[M+H]^+$; ^{1}H-NMR (300 MHz, CD_3OD) δ 7.47-7.42 (m, 2H), 7.23 (dd, J_1 = 9.15 Hz, J_2 = 2.01 Hz, 1H), 4.70 (s, 2H), 2.81 (s, 3H) ppm; ^{13}C-NMR (100 MHz, CD_3OD) δ 183.2, 142.2, 132.8, 130.0, 126.8, 126.5, 125.8, 46.3, 30.6 ppm.

1-(2,4-Dichloro-benzyl)-3-methyl-thiourea (12)
White solid; yield 94%; m.p. 110ºC; IR (KBr) 3256, 3062, 1556, 1297, 1102, 1049, 965, 938, 865, 830, 755 cm^{-1}; FAB-MS (*m/z*): 250 $[M+H]^+$; ^{1}H-NMR (300 MHz, $CDCl_3$) δ 7.42 (d, J = 2.01 Hz, 1H), 7.35-7.25 (m, 2H), 4.76 (s, 2H), 2.95 (s, 3H) ppm; ^{13}C-NMR (75 MHz, $CDCl_3$) δ 173.8, 137.2, 135.6, 135.2, 131.9, 130.8, 128.9, 46.9, 32.0 ppm.

1-Methyl-3-(4-nitro-benzyl)-thiourea (13)
Yellow solid; yield 89%; m.p. 155ºC; IR (KBr) 3378, 3242, 2923, 1571, 1511, 1458, 1348, 1293, 1219, 1174, 1108, 948, 848, 736 cm^{-1}; FAB-MS (*m/z*): 226 $[M+H]^+$; ^{1}H-NMR (300 MHz, DMSO) δ 8.18 (d, J = 8.4 Hz, 2H), 8.07 (s, 1H), 7.67 (s, 1H), 7.51 (d, J = 8.4 Hz, 2H), 4.79 (s, 2H), 2.83 (s, 3H) ppm; ^{13}C-NMR (100 MHz, DMSO) δ 183.7, 148.0, 146.3, 128.6, 1223.8, 46.4, 30.9 ppm.

1-(4-Dimethylamino-benzyl)-3-methyl-thiourea (14)
Yellow solid; yield 47%; m.p. 89ºC; IR (KBr) 3261, 2936, 1615, 1555, 1523, 1345, 1287, 1228, 1190, 1166, 1064, 1018, 947, 807, 752 cm^{-1}; FAB-MS (*m/z*): 223 $[M+H]^+$; ^{1}H-NMR (400 MHz, DMSO) δ 7.73 (s, 1H), 7.33 (s, 1H), 7.13 (d, J = 6.3 Hz, 2H), 6.68 (d, J = 6.45 Hz, 2H), 4.49 (s, 2H), 2.87-2.83 (m, 9H) ppm; ^{13}C-NMR (100 MHz, DMSO) δ 149.7, 128.4, 126.8, 112.4, 46.8, 40.3, 31.2, 30.9 ppm.

1-Methyl-3-(4-methyl-benzyl)-thiourea (15)
White solid; yield 69%; m.p. 116ºC; IR (KBr) 3245, 3021, 2924, 2103, 1557, 1516, 1454, 1344, 1295, 1229, 1083, 1020, 963, 930, 802, 747 cm^{-1}; FAB-MS (*m/z*): 195 $[M+H]^+$; ^{1}H-NMR (300 MHz, $CDCl_3$) δ 7.36-7.21 (m, 4H), 6.29 (s, 2H), 4.67 (s, 2H), 3.02 (d, J = 4.2 Hz, 3H), 2.42 (s, 3H) ppm; ^{13}C-NMR (100 MHz, $CDCl_3$) δ 182.3, 137.6, 133.8, 129.5, 127.5, 48.2, 30.8, 21.0 ppm.

1-Methyl-3-(3-methyl-benzyl)-thiourea (16)
White solid; yield 99%; m.p. 77ºC; IR (KBr) 3254, 3060, 2920, 1607, 1557, 1463, 1341, 1295, 1223, 1081, 1024, 959, 776, 742, 692 cm^{-1}; FAB-MS (*m/z*): 195 $[M+H]^+$; ^{1}H-NMR (300 MHz, $CDCl_3$) δ 7.40-7.33 (m, 2H), 7.24-7.21 (m, 2H), 6.34 (s, 2H), 4.73 (s, 2H), 3.07 (d, J = 4.59 Hz, 3H), 2.46 (s, 3H) ppm; ^{13}C-NMR (100 MHz, $CDCl_3$) δ 182.50, 138.69, 136.91, 128.80, 128.67, 128.33, 124.64, 48.51, 30.88, 21.40 ppm.

1-Methyl-3-(2-methyl-benzyl)-thiourea (17)
White solid; yield 99%; m.p. 90ºC; IR (KBr) 3245, 3064, 1556, 1461, 1344, 1298, 1078, 1020, 962, 746 cm^{-1}; FAB-MS (*m/z*): 195 $[M+H]^+$; ^{1}H-NMR (400 MHz, CD_3OD) δ 7.18-7.14 (m, 4H), 4.60 (s, 2H), 2.86 (s, 3H), 2.27 (s, 3H) ppm; ^{13}C-NMR (100 MHz, CD_3OD) δ 183.25, 137.06, 135.51, 129.90, 126.82, 125.72, 45.28, 30.92, 18.71 ppm.

1-(4-*tert*-Butyl-benzyl)-3-methyl-thiourea (18)
White solid; yield 99%; m.p. 78ºC; IR (KBr) 3255, 2961, 1558, 1515, 1465, 1343, 1295, 1081, 1018, 964, 935, 818, 755 cm^{-1}; FAB-MS (*m/z*): 237 $[M+H]^+$; ^{1}H-NMR (300 MHz, $CDCl_3$) δ 7.37 (d, J = 8.2 Hz, 2H), 7.24 (d, J = 8.1 Hz, 2H), 5.86 (s, 2H), 4.61 (s, 2H), 2.96 (d, J = 4.6 Hz, 3H), 1.3 (s, 9H) ppm; ^{13}C-NMR (100 MHz, $CDCl_3$) δ 182.7, 151.1, 133.7, 127.4, 126.1, 48.3, 34.5, 31.8, 30.8 ppm.

1-(4-Methoxy-benzyl)-3-methyl-thiourea (19)
White solid; yield 57%; m.p. 98°C; IR (KBr) 3256, 2935, 2835, 1612, 1556, 1512, 1463, 1345, 1301, 1248, 1176, 1080, 1032, 963, 819 cm^{-1}; FAB-MS (*m/z*): 211 $[M+H]^+$; ^{1}H-NMR (300 MHz, $CDCl_3$) δ 7.24-7.20 (m , 2H), 6.88-6.83 (m, 2H), 5.98 (s, 2H), 4.55 (s, 2H), 3.77 (s, 3H), 2.94 (d, *J* = 4.59 Hz, 3H) ppm; ^{13}C-NMR (100 MHz, $CDCl_3$) δ 182.18, 159.13, 128.90, 114.12, 55.21, 47.89, 30.76 ppm.

1-Benzo[1,3]dioxol-5-ylmethyl-3-methyl-thiourea (20)
Yellow solid; yield 89%; m.p. 148°C; IR (KBr) 3361, 3198, 3023, 1576, 1525, 1498, 1447, 1365, 1252, 1212, 1038, 936, 822, 636 cm^{-1}; FAB-MS (*m/z*): 225 $[M+H]^+$; ^{1}H-NMR (300 MHz, DMSO) δ 7.84 (s, 1H), 7.46 (s, 1H), 6.88-6.75 (m, 3H), 5.97 (s, 2H), 4.53 (s, 2H), 2.82 (s, 3H) ppm; ^{13}C-NMR (100 MHz, DMSO) δ 183.25, 147.10, 146.01, 133.32, 120.46, 107.92, 100.75, 48.58, 46.68, 30.59 ppm.

1-(2,4-Dimethoxy-benzyl)-3-methyl-thiourea (21)
White solid; yield 85%; m.p. 90°C; IR (KBr) 3264, 2938, 1614, 1589, 1555, 1508, 1463, 1346, 1286, 1208, 1157, 1129, 1081, 10435, 919, 833, 753 cm^{-1}; FAB-MS (*m/z*): 241 $[M+H]^+$; ^{1}H-NMR (300 MHz, CD_3OD) δ 7.18-7.15 (m, 1H), 6.43-6.40 (m, 2H), 4.46 (s, 2H), 3.78 (d, *J* = 12.09 Hz, 6H), 2.93 (s, 3H) ppm; ^{13}C-NMR (100 MHz, CD_3OD) δ 181.7, 160.7, 158.0, 130.6, 117.2, 104.3, 99.4, 55.4, 55.3, 43.3, 31.5 ppm.

1-Methyl-3-(3,4,5-trimethoxy-benzyl)-thiourea (22)
White solid; yield 92%; m.p. 149°C; IR (KBr) 3344, 2939, 2837, 1594, 1556, 1506, 1460, 1423, 1331, 1235, 1181, 1126, 1004, 831, 753 cm^{-1}; FAB-MS (*m/z*): 271 $[M+H]^+$; ^{1}H-NMR (300 MHz, DMSO) δ 7.83 (s, 1H), 7.46 (s, 1H), 6.64 (s, 2H), 4.55 (s, 2H), 3.74 (s, 6H), 3.62 (s, 3H), 2.83 (s, 3H) ppm; ^{13}C-NMR (100 MHz, DMSO) δ 182.8, 152.7, 136.4, 134.9, 104.8, 60.0, 55.8, 47.3, 30.6 ppm.

1-(3,5-Dimethoxy-benzyl)-3-methyl-thiourea (23)
White solid; yield 70%; m.p. 128°C; IR (KBr) 3256, 2938, 2837, 1462, 1430, 1345, 1296, 1204, 1156, 1064, 959, 1833, 751 cm^{-1}; FAB-MS (*m/z*): 241 $[M+H]^+$; ^{1}H-NMR (300 MHz, CD_3OD) δ 6.48 (d, *J* = 2.22 Hz, 2H), 6.35 (t, *J* = 2.22 Hz, 1H), 4.62 (s, 2H), 3.74 (s, 6H), 2.94 (s, 3H) ppm; ^{13}C-NMR (75 MHz, CD_3OD) δ 162.5, 106.3, 100.1, 55.7 ppm.

1-(3-Hydroxy-4-methoxy-benzyl)-3-methyl-thiourea (24)
White solid; yield 64%; m.p. 150°C; IR (KBr) 3334, 1558, 1512, 1439, 1352, 1274, 1128, 1025, 805, 762 cm^{-1}; FAB-MS (*m/z*): 227 $[M+H]^+$; ^{1}H-NMR (300 MHz, CD_3OD) δ 6.82-6.68 (m, 3H), 4.50 (s, 2H), 3.77 (s, 3H), 2.89 (s, 3H) ppm; ^{13}C-NMR (100 MHz, CD_3OD) δ 149.1, 148.4, 120.7, 116.5, 113.5, 57.3 ppm.

1-(3,4-Dihydroxy-benzyl)-3-methyl-thiourea (25)
Yellow solid; yield 58%; m.p. 137°C; IR (KBr) 3430, 1615, 1572, 1512, 1443, 1342, 1288, 1112, 1016, 863, 780, 596 cm^{-1}; FAB-MS (*m/z*): 213 $[M+H]^+$; ^{1}H-NMR (300 MHz, CD_3OD) δ 6.76-6.61 (m, 3H), 4.50 (s, 2H), 2.93 (s, 3H) ppm; ^{13}C-NMR (125 MHz, CD_3OD) δ 183.4, 146.4, 145.7, 131.1, 120.1, 116.2, 115.8, 59.8, 25.8 ppm.

1-Methyl-3-(4-trifluoromethyl-benzyl)-thiourea (26)
Yellow solid; yield 75%; m.p. 90°C; IR (KBr) 3261, 3065, 2925, 1620, 1559, 1420, 1327, 1231, 1165, 1122, 1066, 1018, 968, 941, 820, 751 cm^{-1}; FAB-MS (*m/z*): 249 $[M+H]^+$; ^{1}H-NMR (300 MHz, $CDCl_3$) δ 7.59 (d, *J* = 8.25 Hz, 2H), 7.44 (d, *J* = 8.04 Hz, 2H), 5.98 (s, 2H), 4.81 (d, *J* = 4.95 Hz, 2H), 2.98 (d, *J* = 4.95 Hz, 3H) ppm; ^{13}C-NMR (75 MHz, $CDCl_3$) δ 182.9, 141.5, 130.1, 127.6, 125.6, 122.1, 47.9, 30.7 ppm.

(*S*)-1-[1-(4-Methoxy-phenyl)-ethyl]-3-methyl-thiourea (27)
Yellow solid; yield 99%; m.p. 119°C; IR (KBr) 3255, 2967, 1611, 1552, 1513, 1456, 1344, 1248, 1178, 1107, 1034, 832, 755 cm^{-1}; FAB-MS (*m/z*): 225 $[M+H]^+$; ^{1}H-NMR (300 MHz, CD_3OD) δ 7.24 (d, *J* = 8.61 Hz, 2H), 6.87 (d, *J* = 8.61 Hz, 2H), 5.33 (s, 1H), 3.71 (s, 3H), 2.82 (d, *J* = 4.23 Hz, 3H), 1.37 (d, *J* = 6.78 Hz, 3H) ppm; ^{13}C-NMR (75 MHz, CD_3OD) δ 181.9, 158.0, 136.3, 136.3, 127.2, 113.5, 55.0, 51.7, 30.5, 22.2 ppm.

(*R*)-1-[1-(4-Methoxy-phenyl)-ethyl]-3-methyl-thiourea (28)
Yellow oil; yield 99%; IR (KBr) 3257, 2967, 2835, 1612, 1553, 1513, 1461, 1345, 1248, 1179, 1108, 1034, 833, 755 cm^{-1}; FAB-MS (*m/z*): 225 $[M+H]^+$; ^{1}H-NMR (300 MHz, DMSO) δ 7.17-7.14 (m, 2H), 6.79-6.74 (m, 2H), 5.21 (s, 1H), 3.66 (s, 3H), 2.82 (s, 3H), 1.35 (d, *J* = 6.8 Hz, 3H) ppm; ^{13}C-NMR (75 MHz, DMSO) δ 160.2, 136.9, 128.3, 114.9, 55.7, 53.8, 22.5 ppm.

1-Biphenyl-4-ylmethyl-3-methyl-thiourea (29)
White solid; yield 87%; m.p. 139°C; IR (KBr) 3242, 3054, 1556, 1488, 1343, 1299, 1078, 1009, 940, 846, 762, 696 cm^{-1}; FAB-MS (*m/z*): 257 $[M+H]^+$; ^{1}H-NMR (300 MHz, $CDCl_3$) δ 7.25 (d, *J* = 7.8 Hz, 4H), 7.15-7.02 (m, 5H), 6.02 (s, 2H), 4.40 (s, 2H), 5.65 (d, *J* = 4.23 Hz, 4H) ppm; ^{13}C-NMR (100 MHz, $CDCl_3$) δ 182.5, 140.7, 140.3, 136.0, 128.7, 127.9, 127.4, 127.3, 126.9, 48.1, 30.8 ppm.

1-Methyl-3-(4-pyridin-2-yl-benzyl)-thiourea (30)
Yellow solid; yield 79%; m.p. 109°C; IR (KBr) 3253, 2058, 1557, 1469, 1435, 1343, 1292, 1085, 1015, 965, 940, 777, 751 cm^{-1}; FAB-MS (*m/z*): 258 $[M+H]^+$; ^{1}H-NMR (300 MHz, $CDCl_3$) δ 8.66 (d, *J* = 4.95 Hz, 1H), 7.94 (d, *J* = 8.22 Hz, 2H), 7.78-7.68 (m, 2H), 7.40 (d, *J* = 8.04 Hz, 2H), 7.21 (s, 1H), 6.17 (s, 1H), 5.99 (s, 1H), 4.71 (s, 2H), 2.98 (d, *J* = 4.56 Hz, 3H) ppm; ^{13}C-NMR (100 MHz, $CDCl_3$) δ 182.8, 156.9, 149.3, 138.5, 138.4, 137.0, 127.8, 127.2, 122.2, 120.7, 48.0, 30.9 ppm.

1-(4-Benzyloxy-benzyl)-3-methyl-thiourea (31)
Yellow solid; yield 30%; m.p. 127°C; IR (KBr) 3317, 1610, 1549, 1509, 1453, 1173, 1014, 948, 843, 816, 741, 696 cm^{-1}; FAB-MS (*m/z*): 287 $[M+H]^+$; ^{1}H-NMR (300 MHz, CD_3OD) δ 7.44-7.28 (m, 5H), 7.21 (d, *J* = 8.43 Hz, 2H), 6.97-6.94 (m, 2H), 5.07 (s, 2H), 4.55 (s, 2H), 2.82 (s, 3H) ppm; ^{13}C-NMR (75 MHz, CD_3OD) δ 182.8, 168.9, 157.3, 145.5, 137.2, 131.6, 128.6, 127.7, 114.5, 69.1, 46.4, 31.3 ppm.

1-Methyl-3-(4-phenoxy-benzyl)-thiourea (32)
Yellow solid; yield 65%; m.p. 104°C; IR (KBr) 3254, 1589, 1556, 1505, 1488, 1343, 1237, 1166, 1073, 1017, 871, 753, 692 cm^{-1}; FAB-MS (*m/z*): 273 $[M+H]^+$; ^{1}H-NMR (300 MHz, $CDCl_3$) δ 7.33-7.23 (m, 4H), 7.11-7.06 (m, 1H), 6.98-6.92 (m, 4H), 6.04 (s, 2H), 4.62 (s, 2H), 2.95 (d, *J* = 4.56 Hz, 3H) ppm; ^{13}C-NMR (100 MHz, $CDCl_3$) δ 182.5, 157.1, 156.8, 131.6, 129.8, 129.2, 123.5, 119.0, 48.0, 30.8 ppm.

1-Methyl-3-(3-phenoxy-benzyl)-thiourea (33)
Yellow solid; yield 84%; m.p. 93°C; IR (KBr) 3254, 3062, 1574, 1556, 1487, 1444, 1341, 1252, 1213, 1163, 1073, 1023, 965, 758, 691 cm^{-1}; FAB-MS (*m/z*): 273 $[M+H]^+$; ^{1}H-NMR (400 MHz, CD_3OD) δ 7.33-7.25 (m, 3H), 7.09-7.05 (m, 2H), 6.97-6.95 (m, 3H), 6.83 (dd, J_1 = 6.44 Hz, J_2 = 1.48 Hz, 1H), 4.68 (s, 2H), 2.92 (s, 3H) ppm; ^{13}C-NMR (100 MHz, CD_3OD) δ 184.8, 159.6, 159.4, 143.2, 131.6, 125.2, 124.0, 120.7, 120.0, 119.5, 119.2, 42.3, 34.3 ppm.

1-Methyl-3-(4-*o*-tolyloxy-benzyl)-thiourea (34)
Yellow solid; yield 24%; m.p. 156°C; IR (KBr) 3230, 3063, 1557, 1486, 1453, 1343, 1233, 1075, 875, 752, 691 cm^{-1}; FAB-MS (*m/z*): 273 $[M+H]^+$; ^{1}H-NMR (300 MHz, CD_3OD) δ 7.40-7.31 (m, 3H), 7.26-7.21 (m, 1H), 7.13-7.06 (m, 2H), 6.98-6.95 (m, 2H), 6.85-6.82 (m, 1H), 4.72 (s, 2H), 2.90 (s, 3H) ppm; ^{13}C-NMR (75 MHz, CD_3OD) δ 158.9, 156.0, 130.9, 130.4, 129.7, 125.2, 124.8, 124.2, 119.9, 119.2, 54.8, 44.1 ppm.

1-[4-(4-Fluoro-phenoxy)-benzyl]-3-methyl-thiourea (35)
Yellow oil; yield 67%; IR (KBr) 3254, 3062, 1557, 1496, 1334, 1250, 1213, 1192, 1167, 1089, 1013, 964, 876, 831 cm^{-1}; FAB-MS (*m/z*): 291 $[M+H]^+$; ^{1}H-NMR (300 MHz, $CDCl_3$) δ 7.28-7.26 (m, 2H), 7.05-6.91 (m, 6H), 5.91 (s, 2H), 4.63 (d, *J* = 4.74 Hz, 2H), 2.97 (d, *J* = 4.95 Hz, 3H) ppm; ^{13}C-NMR (100 MHz, CD_3OD) δ 161.9, 160.0, 159.0, 155.4, 130.9, 122.3, 120.1, 118.1, 118.0, 62.3, 21.7 ppm.

1-[4-(4-Methoxy-phenoxy)-benzyl]-3-methyl-thiourea (36)
Yellow solid; yield 84%; m.p. 102°C; IR (KBr) 3255, 2939, 1556, 1499, 1464, 1344, 1295, 1227, 1101, 1033, 964, 875, 842, 753 cm^{-1}; FAB-MS (*m/z*): 303 $[M+H]^+$; ^{1}H-NMR (400 MHz, $CDCl_3$) δ 7.24-7.20 (m, 2H), 6.93-6.84 (m, 6H), 6.15 (s, 2H), 4.58 (s, 2H), 2.93 (s, 3H) ppm; ^{13}C-NMR (100 MHz, $CDCl_3$) δ 182.4, 158.3, 15630, 149.6, 128.8, 121.1, 117.8, 117.2, 114.9, 55.6, 48.0 ppm.

1-Methyl-3-naphthalen-2-ylmethyl-thiourea (37)
N-Methyl thiourea (180.3 mg, 2.00 mmol) was added to a stirred solution of 2-bromomethyl naphthalene (221.1 mg, 1.00 mmol) in MeOH (4 mL). After stirring for 2 h, the reaction mixtures was evaporated and diluted with EtOAc (50 mL), washed with brine (20 mL), dried over anhydrous $MgSO_4$, filtered, and concentrated *in vacuo*. The residue was purified by column chromatography (silica gel, EtOAc-MeOH = 10:1) to afford **37** (131.3 mg) as white solid; yield 57%; m.p. 97°C; IR (KBr) 3052, 1650, 1603, 1508, 1413, 1165, 1019, 860, 820, 754 cm^{-1}; FAB-MS (*m/z*): 231 $[M+H]^+$; ^{1}H-NMR (400 MHz, DMSO) δ 9.27 (s, 1H), 7.91-7.86 (m, 5H), 7.55-7.51 (m, 3H), 4.71 (s, 2H), 2.83 (s, 3H) ppm; ^{13}C-NMR (100 MHz, DMSO) δ 163.2, 133.7, 132.7, 132.2, 128.3, 128.1, 128.0, 127.6, 126.9, 126.2, 34.71, 30.5 ppm.

Biological assay

HepG2 cells obtained from the American Type Culture Collection were maintained at 37°C in 5% CO_2 in Dulbecco's Modification of Eagle's Medium with 10% fetal bovine serum. HepG2 cells were plated at a density of 1×10^5 cells per well of a 12-well plate and were transfected with RORE-*tk*-Luc plasmid using Welfect-EX™ PLUS (WelGENE Inc.). After transfection, cells were treated with increasing concentration of compound **1** (lead compound) or **32** (a derivative); from 1 to 100 (μM). Reporter gene analysis was as previously described (Kim et al., 2008).

Molecular modeling

For the docking study of **32** into the binding site of

RORα, Surflex-Dock was used as the docking algorithm in Sybyl version 8.1.1 (Tripos Associates), which was operated under Red Hat Linux 4.0 on an IBM computer (Intel Pentium 4, 2.8 GHz CPU, 1GB memory). As the binding site of RORα from the given RORα-cholesterol sulfate complex structure (PDB# 1S0X) was prepared to give a protomol, the chemical structure of **32** was also prepared using the Sybyl package with standard bond lengths and angles. The structure was minimized through the conjugate gradient method by applying Gasteiger-Huckel charge with a distance-dependent dielectric function. The Surflex-Dock performed the docking to the protomol, which represents the ligand-binding pocket of RORα, and the protomol is critical and essential for docking since it elucidates potential interactions with the site allowing for rapid docking of ligands into simplistic representations of the site. As a result of the Surflex-Dock of **32**, twenty conformers were aligned in a high scoring sequence, and the best scoring conformer was selected to further investigate the binding mode of the ligand to the active site.

RESULTS AND DISCUSSIONS

Thirty two N-methylthiourea derivatives were easily prepared in one step from the corresponding amines or aldehydes (Scheme 1). All compounds gave satisfactory spectroscopic data consistent with the proposed structures. The coupling of methylisocynate with various benzylic amines **3** gave the corresponding N-methylthioureas (**6**-**28**). The formation of imine from aldehydes **4** and N-methylthiourea in the presence of $Ti(OiPr)_4$ under THF, followed by reduction with $NaBH_4$ provided the corresponding N-methylthioureas (**29**-**37**) (Armstrong et al., 1997).

The RORα agonistic activities of the prepared derivatives were evaluated based on transcription activity

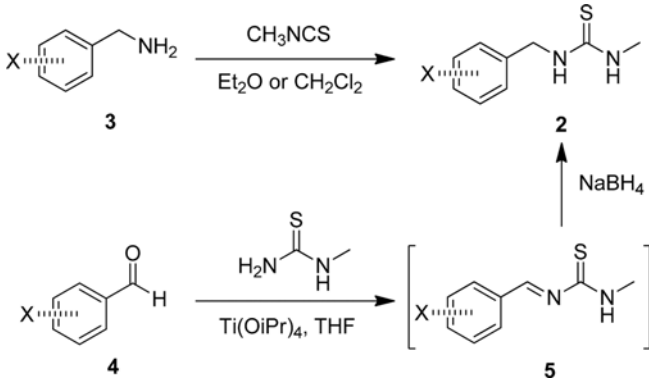

Scheme 1. General procedure for preparation of N-methylthioureas.

using HepG2 cells transfected with RORE-Luc, as described previously (Kim et al., 2008). The fold activation in the presence of test compounds was compared with that of no treatment. As shown in Table I, most of thiourea derivatives induced transcriptional activity of RORα. The agonistic activity was not sensitive to the nature of the functional groups; however, the substituted position was important to their biological activity. Generally, *para*-substitutents showed higher agonistic activity than the corresponding *meta*- or *ortho*-substitutents. Further substitution at the *meta*- and *ortho*-position in addition to the *para*-position led to a significant decrease of activity. Some *para*-substituted electron donating groups exhibited high agonistic activity (**15**, 4-CH_3, 3.9; **19**, 4-CH_3O, 3.4) except for the bulky groups (**14**, $(CH_3)_2N$, 1.3; **18**, *tert*-butyl, 0.9). A large loss of activity was observed for the methylated analogues of **19** (*R*-**27**, 0.7; *S*-**28**, 0.6) at benzylic position, which implies that the agonistic activity is quite sensitive to the conformation. The biphenyl derivative (**29**, 0.2) had the lowest agonistic activity, but high activity was observed for the 2'-pyridyl analogue (**30**, 1.9). The ether linkage analogue showed the highest agonistic activity (**32**, 4.6). A similar decreases in activity were observed for the *meta*- and *ortho*-analogues (**33**, 1.0; **34**, 1.3). The cumulative results indicate that the binding pocket of RORα is not spacious but rather linear. Unfortunately, a further increase in activity by substitution of functional group at **32** was not observed (**35**, 1.5; **36**, 2.1).

We chose two of the highest effective agonists **31** and **32** in activating RORE-Luc and examined the transcriptional activity depending on the concentration along with CGP52608 (**1**). The RORα transcriptional activity of CGP52608 (**1**) was lower than that of the previous report (Wiesenberg et al., 1995), which might be due to the less sensitivity of our assay system. The transcriptional activity was clearly proportional to the concentration of **31** and **32** (Fig. 2).

To examine the docking of the most effective agonist **32** into the ligand-binding pocket of RORα, the X-ray crystal structure of RORα complex with cholesterol sulfate (PDB# 1S0X) was applied (Kallen et al., 2002). The binding site of RORα contains two characteristic regions: hydrophilic and hydrophobic areas in which some amino residues interact with the functional groups of **32** (Fig. 3). In terms of hydrophilic interactions, two hydrogen bonds between each NH of thiourea in **32** and the carbonyl oxygen of Gln 289 were observed. In terms of hydrophobic interactions, the phenoxy benzene ring of **32** was thoroughly enclosed with residues Cys 323, Ile 327, Ala 330, Phe 365 and Phe 381 of the lipophilic pocket, suggesting that compound **32** fit well

Table I. *In vitro* biological activity of the N-methylthioureas in the RORα transcriptional assay

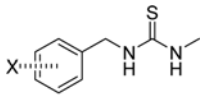

2

Compound No.	X	Fold activation[a]	Compound No.	X	Fold activation
6		1.5	**22**	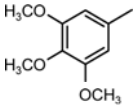	2.2
7	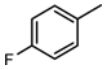	2.5	**23**	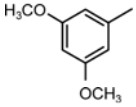	1.0
8	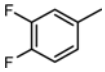	0.8	**24**	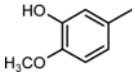	1.9
9	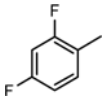	0.9	**25**	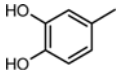	0.6
10	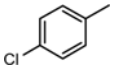	2.6	**26**	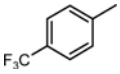	2.3
11	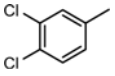	1.0	**27**	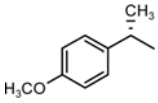	0.7
12	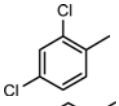	0.6	**28**	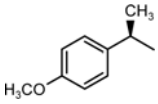	0.6
13	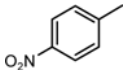	1.6	**29**	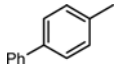	0.2
14	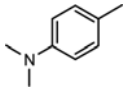	1.3	**30**	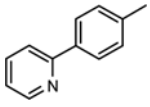	1.9
15	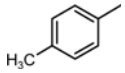	3.9	**31**	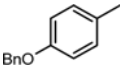	3.6
16	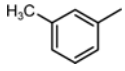	1.1	**32**	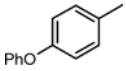	4.8
17		0.7	**33**	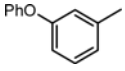	1.0
18	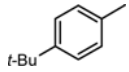	0.9	**34**		1.3
19	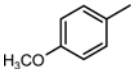	3.4	**35**	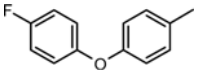	1.5
20	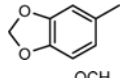	1.7	**36**	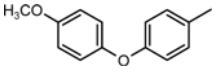	2.1
21	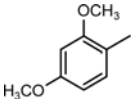	1.1	**37**	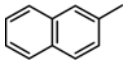	0.7

[a]Fold activation of the derivative was the ratio of activating activity of RORE-Luc in the presence of derivative (100 mM) compared to that of no treatment15 and fold activation values were estimated from 3 times replicates [$p < 0.01$ *vs* vehicle (n = 3)].

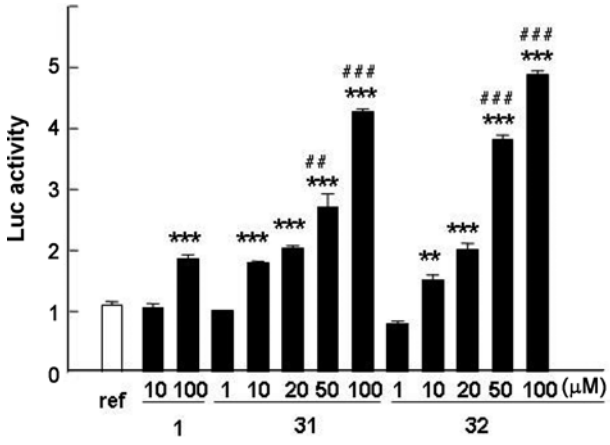

Fig. 2. RORα transcriptional activity of **31** and **32**. HepG2 cells were transfected with the RORE-Luc and treated with compounds (**31** and **32**). $^{**}p < 0.01$ and $^{***}p < 0.001$ *vs* vehicle; $^{\#\#}p < 0.01$ and $^{\#\#\#}p < 0.001$ *vs* **1** (100 μM) (n = 3).

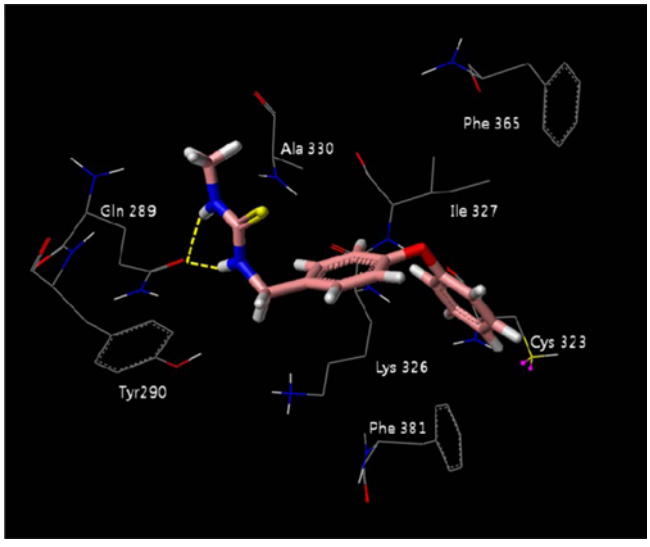

Fig. 3. The H-bond mode of **32** docked with amino acids in the binding site of RORα.

into the binding site of RORα.

In conclusion, thirty two thiourea derivatives were prepared and their agonistic activities against RORα were evaluated. A significant increase in agonistic activities were observed by replacing the 3-allyl-2-imino-thiazolidin-4-one moiety of the lead compound CGP52608 (**1**) with substituted phenyl rings. Among them, 1-methyl-3-(4-phenoxy-benzyl)-thiourea (**32**) showed the best agonistic activity. We believe this pharmacophore information would be very useful in the design of more potent agonistic scaffolds for the treatment of metabolic disorders such as fatty liver diseases. The further focused structure-activity relationship study is now under investigation.

ACKNOWLEDGEMENTS

This work was supported by the National Research Foundation (NRF) grant funded by the Korea government (MEST) (No. 201000017).

REFERENCES

Armstrong, J. D., III, Wolfe, C. N., Keller, J. L., Lynch, J., Bhupathy, M., Volante, R. P., and De Vita, R. J., A novel synthesis of disubstituted ureas using titanium (IV) isopropoxide and sodium borohydride. *Tetrahedron Letts.*, 38, 1531-1532 (1997).

Becker-Andre, M., Andre, E., and DeLamarter, J. F., Identification of nuclear receptor mRNAs by RT-PCR amplification of conserved zinc-finger motif sequences. *Biochem. Biophys. Res. Commun.*, 194, 1371-1379 (1984).

Carlberg, C., Hooft van Huijsduijnen, R., Staple, J. K., DeLamarter, J. F., and Becker-Andre, M., RZRs, a new family of retinoid-related orphan receptors that function as both monomers and homodimers. *Mol. Endocrinol.*, 8, 757-770 (1994).

Eberl, G. and Littman, D. R., The role of the nuclear hormone receptor RORgammat in the development of lymph nodes and Peyer's patches. *Immunol. Rev.*, 195, 81-90 (2003).

Giguere, V., Tini, M., Flock, G., Ong, E., Evans, R. M., and Otulakowski, G., Isoform-specific amino-terminal domains dictate DNA-binding properties of ROR alpha, a novel family of orphan hormone nuclear receptors. *Genes Dev.*, 8, 538-553 (1994).

Giguere, V., Beatty, B., Squire, J., Copeland, N. G., and Jenkins, N. A., The orphan nuclear receptor ROR alpha (RORA) maps to a conserved region of homology on human chromosome 15q21-q22 and mouse chromosome 9. *Genomics,* 28, 596-598 (1995).

Gold, D. A., Baek, S. H., Schork, N. J., Rose, D. W., Larsen, D. D., Sachs, B. D., Rosenfeld, M. G., and Hamilton, B. A., RORalpha coordinates reciprocal signaling in cerebellar development through sonic hedgehog and calcium-dependent pathways. *Neuron,* 40, 1119-1131 (2003).

He, Y. W., Deftos, M. L., Ojala, E. W., and Bevan, M. J., RORgamma t, a novel isoform of an orphan receptor, negatively regulates Fas ligand expression and IL-2 production in T cells. *Immunity,* 9, 797-806 (1998).

He, Y. W., Orphan nuclear receptors in T lymphocyte development. *J. Leukoc. Biol.*, 72, 440-452 (2002).

Hirose, T., Smith, R. J., and Jetten, A. M., ROR gamma: the third member of ROR/RZR orphan receptor subfamily that is highly expressed in skeletal muscle. *Biochem. Biophys. Res. Commun.*, 205, 1976-1983 (1994).

Jetten, A. M., Kurebayashi, S., and Ueda, E., The ROR nuclear orphan receptor subfamily: critical regulators of multiple biological processes. *Prog. Nucl. Acid Res.*, 69, 205-247 (2001).

Jetten, A. M. and Ueda, E., Retinoid-related orphan receptors

(RORs): roles in cell survival, differentiation and disease. *Cell Death Differ.*, 9, 1167-1177 (2002).

Jetten, A. M., Recent advances in the mechanisms of action and physiological functions of the retinoid-related orphan receptors (RORs). *Curr. Drug Targets Inflamm. Allergy*, 3, 395-412 (2004).

Kallen, J. A., Schlaeppi, J. M., Bitsch, F., Geisse, S., Geiser, M., Delhon, I., and Fournier, B., X-ray structure of the hRORalpha LBD at 1.63 A: structural and functional data that cholesterol or a cholesterol derivative is the natural ligand of RORalpha. *Structure*, 10, 1697-1707 (2002).

Kallen, J., Schlaeppi, J. M., Bitsch, F., Delhon, I., and Fournier, B., Crystal structure of the human RORalpha Ligand binding domain in complex with cholesterol sulfate at 2.2 A. *J. Biol. Chem*., 279, 14033-14038 (2004).

Kim, E. J., Yoo, Y. G., Yang, W. K., Lim, Y. S., Na, T. Y., Lee, I. K., and Lee, M.-O., Transcriptional activation of HIF-1 by RORalpha and its role in hypoxia signaling. *Arterioscler. Thromb. Vasc. Biol.*, 28, 1796-1802 (2008).

Lau, P., Fitzsimmons, R. L., Raichur, S., Wang, S. C., and Lechtken, A., The orphan nuclear receptor, RORalpha, regulates gene expression that controls lipid metabolism: staggerer (SG/SG) mice are resistant to diet-induced obesity. *J. Biol. Chem*., 283, 18411-18421 (2008).

Medvedev, A., Yan, Z. H., Hirose, T., Giguere, V., and Jetten, A. M., Cloning of a cDNA encoding the murine orphan receptor RZR/ROR gamma and characterization of its response element. *Gene,* 181, 199-206 (1996).

Meyer, T., Kneissel, M., Mariani, J., and Fournier, B., *In vitro* and *in vivo* evidence for orphan nuclear receptor RORalpha function in bone metabolism. *Proc. Natl. Acad. Sci. U. S. A.*, 97, 9197-9202 (2000).

Missbach, M., Jagher, B., Sigg, I., Nayeri, S., Carlberg, C., and Wiesenberg. I., Thiazolidine diones, specific ligands of the nuclear receptor retinoid Z receptor/retinoid acid receptor-related orphan receptor alpha with potent antiarthritic activity. *J. Biol. Chem*., 271, 13515-13522 (1996).

Ortiz, M. A., Piedrafita, F. J., Pfahl, M., and Maki, R., TOR: a new orphan receptor expressed in the thymus that can modulate retinoid and thyroid hormone signals. *Mol. Endocrinol.*, 9, 1679-1691 (1995).

Raspe, E., Duez, H., Gervois, P., Fievet, C., Fruchart, J. C., Besnard, S., Mariani, J., Tedgui, A., and Staels, B., Transcriptional regulation of apolipoprotein C-III gene expression by the orphan nuclear receptor RORalpha. *J. Biol. Chem.*, 276, 2865-2871 (2001).

Steinhilber, D., Brungs, M., Werz, O., Wiesenberg, I., Danielsson, C., Kahlen, J.-P., Nayeri, S., Schrader, M., and Carlberg, C., The nuclear receptor for melatonin represses 5-lipoxygenase gene expression in human B lymphocytes. *J. Biol. Chem*., 270, 7037-7040 (1995).

Vu-Dac, N., Gervois, P., Grötzinger, T., De Vos, P., Schoonjans, K., and Fruchart, J. C., Transcriptional regulation of apolipoprotein A-I gene expression by the nuclear receptor RORalpha. *J. Biol. Chem*., 272, 22401-22404 (1997).

Wada, T., Kang, H. S., Jetten, A. M., and Xie, W., The emerging role of nuclear receptor RORalpha and its crosstalk with LXR in xeno- and endobiotic gene regulation. *Exp. Biol. Med*., 233, 1191-1201 (2008).

Wang. Y., Solt, L. A., and Burris, T. P., Regulation of FGF21 expression and secretion by retinoic acid receptor-related orphan receptor alpha. *J. Biol. Chem*., 285, 15668-15673 (2010).

Wiesenberg, I., Missbach, M., Kahlen, J.-P., Schraeder, M., and Carlberg, C., Transcriptional activation of the nuclear receptor RZR alpha by the pineal gland hormone melatonin and identification of CGP 52608 as a synthetic ligand. *Nucleic Acids Res*., 23, 327-333 (1995).